# Laser-Induced Protein–DNA Cross-Links via Psoralen Furanside Monoadducts†

Srinivas S. Sastry,‡,§ H. Peter Spielmann,‡ Quan Scott Hoang,‡ A. Meleah Phillips,∥ Aziz Sancar,∥ and John E. Hearst*,‡

*Department of Chemistry, University of California, Berkeley, Division of Chemical Biodynamics, Lawrence Berkeley Laboratory, Berkeley, California 94720, and Department of Biochemistry, University of North Carolina, Chapel Hill, North Carolina 27599*

*Received November 2, 1992; Revised Manuscript Received March 10, 1993*

ABSTRACT: We have developed a technique for cross-linking DNA binding proteins to DNA using psoralen furanside monoadducts as photoaffinity probes and a continuous-wave argon ion laser (366 nm) as a light source. Several DNA binding proteins (T7 RNA polymerase, UvrB, single-stranded DNA binding protein of *Escherichia coli*, T4 gp32, and RecA of *E. coli*) are shown to cross-link to single-stranded psoralen monoadducted DNA oligos differing in length and sequence. Increasing fluences of laser light on a fixed ratio of DNA/protein resulted in an increase in the yield of cross-links. Titration experiments were carried out to measure the apparent cross-linking constant ($K_{appXL}$) for T7 RNA polymerase or UvrB to a monoadducted 24 mer DNA. The estimated values for the apparent cross-linking constant were in the range of (2–3) × $10^{-7}$ M for both T7 RNA polymerase and UvrB. The efficiency of cross-linking was investigated as a function of the length of adducted DNA and also as a fraction of the total noncovalent binding of proteins of psoralenated DNAs. The results showed that in the cases of T7 RNA polymerase and UvrB cross-linking was more efficient with short oligos (8 and 19 mers) as compared to longer oligos (50 mer). A tryptic peptide of T7 RNA polymerase that was conjugated to a psoralen furanside monoadducted 12 mer DNA was isolated by high-performance liquid chromatography. Mass spectrometry and amino acid composition of this peptide revealed that it originated from a region between residues 558 and 608 of the primary structure of T7 RNA polymerase. Two other peptides cross-linked to oligos were also purified. Repeated attempts to perform Edman sequencing of the peptide–DNA conjugates failed. Overall evidence indicates that photo-cross-linking of furanside monoadducts occurred at multiple sites on the proteins. We have shown that T7 RNA polymerase molecules in a ternary complex arrested at the furanside monoadduct can be cross-linked to the DNA templates with laser light. Evidence suggests that the arrested polymerase molecules existed in multiple conformations on the DNA template. This method of transcriptional cross-linking offers a new method for preparing highly stable elongation complexes for further studies.

Protein–DNA interactions play a crucial role in the regulation of gene activity. One major advance in the understanding of protein–DNA interactions has been the introduction of chemical and photochemical cross-linking of proteins to DNA or RNA. The techniques of cross-linking proteins to nucleic acids are complementary to nucleic acid "footprinting" methods, which give a more general picture of the DNA contacts between proteins and nucleic acids. Covalent cross-linking of proteins to nucleic acids stabilizes macromolecular interactions against denaturing conditions, thereby providing a powerful handle for the researcher to purify the covalent complexes away from other unbound components in the reaction mixture. This allows one to identify the microscopic contacts between the relevant amino acids and nucleotides and offers an opportunity for a rigorous chemical description of the nature of these contacts. Covalent cross-linking of proteins to DNA (or RNA) by short-wave (254 nm) UV, usually emitted from a germicidal lamp, has gained a great deal of popularity because of the simplicity of this procedure [for reviews, see Smith (1977), Shetlar et al. (1984), Shetlar (1981), and Hockensmith et al. (1991)]. This UV wavelength is close to the absorption maxima of DNA, RNA, and some amino acid side chains. The numbers of studies that have utilized this technique are too numerous to mention here [for review, see Williams and Konigsberg (1991)], but some of the more notable ones include the following: cross-linking of DNA and RNA polymerases to their template DNAs (Markovitz, 1972; Strniste & Smith, 1974; Hillel & Wu, 1978; Harrison et al., 1982), cross-linking histones to DNA in nucleosomes (Kunkel & Martinson, 1978); several single-stranded binding proteins to ssDNA (Merrill et al., 1984; Paradiso & Konigsberg, 1982; Lica & Ray, 1977); tRNA synthetases to tRNA (Budzik et al., 1975); and ribosomal proteins to rRNA (Gorelic, 1975a,b; Moller & Brimacombe, 1975; Reboud et al., 1978). In only a few instances has the exact nature of the UV cross-linking site (nucleic acid base–amino acid side chain) been identified [for review, see Williams and Konigsberg (1991)].

We describe a procedure in which psoralen furanside monoadducted DNA oligonucleotides are cross-linked to single- and double-stranded DNA binding proteins with argon ion laser light at 366 nm. This wavelength is well away from the absorption maximum of both DNA and most proteins. We have extended this technique to include the formation of adducts between T7 RNA polymerase and its DNA template in a ternary complex arrested at a furanside monoadduct. Psoralens are linear bifunctional furocoumarins that have been used for the treatment of vitiligo, psoriasis, and other cutaneous

† This work was supported by the Director, Office of Energy Research, Office of General Life Sciences, Molecular Biology Division of the U.S. Department of Energy under Contract No. DE-AC03-76SF00098 and NIH Grant GM 41911 to J.E.H. S.S.S. was supported by Grant NIEHS 07075-11. Support was also received from NIH Grant GM 32833 to A.S.

* Author to whom correspondence should be addressed.

‡ Department of Chemistry, University of California, Berkeley, and Division of Chemical Biodynamics, Lawrence Berkeley Laboratory.

§ Present address: Founder's Hall, Rm. 215, P.O. Box 400, The Rockefeller University, 1230 York Avenue, New York, NY 10021-6399.

∥ Department of Biochemistry, University of North Carolina.

0006-2960/93/0432-5526$04.00/0 

diseases [see Pathak and Fitzpatrick (1992) for a review]. Psoralens react efficiently with DNA or RNA to form a set of well-characterized covalent adducts when exposed to long-wavelength UV light (UV-A = 310–400 nm). Psoralens react primarily with thymidine and to a lesser extent with cytosine in DNA to form cyclobutane adducts [see Cimino et al. (1985) for review]. In contrast to nucleic acids, the reactivity of psoralens with proteins is extremely poor and is highly dependent on the chemical structure of the psoralen [Musajo & Rodighiero, 1972; Yoshikawa et al., 1979; see Midden (1988) for a review]. The mechanism by which psoralens photobind to proteins is poorly understood. Psoralens have been shown to photochemically inactivate a number of enzymes (Midden, 1988). Some examples are lysozyme, glutamate dehydrogenase, 6-phosphogluconate dehydrogenase (Veronese et al., 1982; Schiavon & Veronese, 1986), and ribonuclease (Schiavon et al., 1984). In these studies, several different amino acids in the proteins were shown to react with free psoralens.

There have been only a few reports in which psoralens have been used to cross-link DNA to proteins. Cantor and his colleagues have used derivatized psoralens with linker arms to form protein–DNA cross-links (Schwartz et al., 1983). The disadvantage of these reagents has been their poor photoreactivity and the unidirectionality of the cross-linking reaction. This unidirectionality is dictated by the initial attachment of a tethered psoralen to a protein and subsequent cross-linking of the derivatized protein conjugate to the target DNA using long-wave UV light. This method is not generally applicable to all DNA binding proteins because some of these molecules may be inactivated or have their nucleic acid binding properties altered by the initial derivitization. In another study, psoralen monoadducted DNAs were shown to photoreact in an oxygen-dependent manner with a synthetic tetrapeptide (Morliere et al., 1986).

Here we demonstrate the general ability of psoralen furanside monoadducted DNA oligos to cross-link several DNA binding proteins. We show that T7 RNA polymerase can be cross-linked to its template DNA in an arrested ternary complex. This technique is used to probe the contacts between DNA and T7 RNA polymerase. Several tryptic fragments of T7 RNA polymerase covalently cross-linked to monoadducted DNA oligos were purified by HPLC.[1] Evidence indicates that there are multiple sites on the proteins for the photo-cross-linking of psoralen monoadducts. The molecular mass of a partial tryptic fragment of T7 RNAP that was cross-linked to the psoralen was determined by laser desorption mass spectrometry, and a portion of the DNA binding domain of T7 RNAP is proposed to account for the origin of this peptide.

## MATERIALS AND METHODS

*DNAs and Proteins.* DNA oligonucleotides were synthesized on an Applied Biosystems automated DNA synthesizer by David Koh (Lawrence Berkeley Laboratory, Berkeley). HMT and $^3$H-HMT (sp act. 17 000 Ci/mol) were a gift of HRI Associates, Inc., (Concord, CA). Stock solutions of HMT (~0.5 M) were prepared in dimethyl sulfoxide. Argon ion and krypton ion lasers were manufactured by Spectra-Physics (Mountain View, CA). Quartz flow cells were supplied by NSG Precision Cells Inc. (Farmingdale, NY). HPLC instrumentation was purchased from Beckman (Palo Alto, CA) and Rainin Instruments (Emeryville, CA). The Dynamax C18 reverse-phase HPLC column and the Hydropore-SAX anion-exchange column were purchased from Rainin Instruments (Emeryville, CA). An Aquapore C8 narrow-bore HPLC column was purchased from Applied Biosystems (Foster City, CA). HMT furanside monoadducts of the DNA oligos (except for the 50 mer) used in this work were synthesized and purified on HPLC by methods described elsewhere (Spielmann et al., 1992; Sastry et al., 1992). The oligo furanside monoadducts and their unmodified parental DNAs were 5′ end labeled with T4 polynucleotide kinase and [$\gamma$-$^{32}$P]ATP (Maniatis et al., 1982). Unicorporated radioactivity was removed by purification of the labeled oligos on SEP-PAK C18 cartridges (procedure from Waters Associates, MA). All enzymes for routine DNA manipulations were obtained from New England Biolabs (MA). T7 RNA polymerase was a gift of Chris Noren (Department of Chemistry, UC, Berkeley). UvrB was prepared as described previously (Thomas et al., 1985). RecA protein of *Escherichia coli* and phage T4 gp32 were purchased from Pharmacia (Piscataway, NJ).

*Irradiation of Protein–DNA Reactions with a Continuous-Wave Argon Ion Laser.* Various proteins and $^{32}$P-labeled DNA oligos were mixed in 50 $\mu$L of irradiation buffer, which consisted of 50 mM Tris-HCl, pH 8.0, 10 mM $MgCl_2$, 1 mM DTT, 0.5 mM spermidine, and 5% glycerol, in plastic Eppendorf tubes. For reactions involving RecA protein, the buffer used was 65 mM potassium acetate, 10 mM magnesium acetate, 10 mM Tris–acetate, pH 7.4, 0.5 mM spermine, 0.3 mM spermidine, and 10 mM DTT. Proteins were added to labeled DNA oligos in buffer, and the reactions were incubated at room temperature (~25 °C) for 10 min and then transported to the laser room (total incubation time was 15 min). Irradiations at room temperature (22–23 °C) were carried out with a Spectra-Physics 2045 Argon laser operating in broad band mode centered at 366 nm. The tubes containing the reactions were positioned in the path of the laser light [as described by Spielmann et al. (1992)]. To minimize tube to tube variations in focal positioning, the Eppendorf tubes were always placed in a cuvette holder so that the light beam is directed at the same place on the tube. A cylindrical quartz lens was used to broaden the laser light beam to illuminate the entire area of the reaction solution. The output of the laser was adjusted to give ~$4.6 \times 10^{18}$ photons $s^{-1}$ $cm^{-2}$ at the irradiation surface. This corresponded to a power output of 2.5 W from the laser. The samples were irradiated for 10 s by controlling the laser shutter.

*Irradiation of Protein–DNA Mixtures with a Black Light Lamp.* Protein–DNA mixtures were prepared as described above in Eppendorf plastic tubes. The tubes, with their caps open, were placed in a tube rack that was covered with a Pyrex glass plate to block short-wave UV. The tube rack was placed in an ice bath to prevent excessive heating of the tubes during irradiation. The irradiation was carried out for 30 min using a bank of black light lamps (Southern New England Ultraviolet Co.; $\lambda_{max}$ = 360 nm; 2 mW $cm^{-2}$) arranged in parallel in a housing. The lamps were at a height of 10 cm from the top of the Eppendorf tubes. After the irradiations,

[1] Abbreviations: amu, atomic mass units; HMT, 4′-hydroxymethyl-4,5′,8-trimethylpsoralen; UM, unmodified; MAf, monoadduct furanside; XL, cross-link; BSA, bovine serum albumin; rNTP(s) ribonucleoside triphosphates; DTT, dithiothreitol; EDTA ethylenediaminetetraacetic acid; nt(s), nucleotide(s); kbp, kilobase pairs; kDa, kilodaltons; ss, single-stranded, ds, double-stranded; NMR, nuclear magnetic resonance; ATP, adenosine triphosphate; ATP$\gamma$S, adenosine 5′-*O*-(3-thiophosphate); GpG, guanylyl 3′–5′-guanosine; T7 RNAP, bacteriophage T7 RNA polymerase; SSB, single-stranded binding protein of *E. coli*; UvrB, a subunit of the complex of ultraviolet light-induced DNA-damage repair proteins of *E. coli*; HPLC, high-performance liquid chromatography; SAX, strong anion exchange; TFA, trifluoroacetic acid.

the reaction mixtures were processed for electrophoresis as described below.

*Electrophoresis of the Products of Irradiation.* Following irradiation, the reaction mixture was lyophilized to semi-dryness in a speedvac (Savant). The residue was resuspended in 8 M urea + 1X SDS–sample dyes (30 μL) and heated in a boiling water bath for 5–10 min. The samples were run on 12.5% polyacrylamide–SDS gels (Laemmli, 1970). Gels were 15 cm (width) × 20 cm (length) × 1.5 mm (thickness) and run at 12 mA for 18 h until the bromophenol blue ran off the gel. Gels were fixed in 5% acetic acid + 5% methanol + 3% glycerol, dried, and autoradiographed with Kodak X-omat AR film. Sometimes the proteins on the gels were also visualized either with Coomassie Brilliant Blue R250 or with silver stain depending on the amount of protein loaded on the gels. All gels contained prestained protein gel markers (Bio-Rad Labs, Hercules, CA) to enable comparisons with the position of bands on the autoradiograms. For the purposes of quantification of the gel bands, autoradiography was also performed with a PhosphorImager (Molecular Dynamics Corp., Sunnyvale, CA). Gel bands were scanned by PhosphorImager using the Image-Quant program, and the integrated areas of the bands representing protein–DNA complexes and free DNA were compared. In many of the gels shown in this paper, some of the free DNA was run off the gel. This was necessitated because the presence of excess free DNA in the gel caused the background $^{32}P$ on the gel to increase during fixation of the gels. All the gel photographs shown in this paper were obtained from X-ray film, since this method gave better quality images of gels than PhosphorImaging.

*Nitrocellulose Filter Binding Assay for Protein Binding to DNAs.* Nitrocellulose filters (13 mm diameter, 0.45 μm, BA85; Schliecher and Schuell, Keene, NH) were soaked in 1X irradiation buffer (see above for composition) at room temperature (~25 °C). The filters were mounted on a filtration apparatus and washed with 2 mL of irradiation buffer. For the assay of noncovalent binding, duplicate reaction samples (50 μL) were incubated at room temperature for 15 min and applied to the filters, and suction was applied (flow rate with house vacuum was adjusted to ~1 mL/min). The filters were then washed with 1 mL of irradiation buffer. The radioactivity on the filters was measured with added scintillation fluor (ReadySafe, Beckman) in a liquid scintillation counter. To measure covalent photoaddition, samples were prepared exactly as described above except that they were irradiated with argon laser light (366 nm), denatured in 1% SDS and 8 M urea, and heated in a boiling water bath (see above). These samples were then applied to nitrocellulose filters and washed as described in the assay for noncovalent binding. Mock reactions, i.e., identical samples that were not laser irradiated but denatured by heating in 1% SDS–8 M urea, served as controls. The number of $^{32}P$ counts per minute retained on the filters for the control reactions was subtracted from the experimental values obtained for irradiated and nonirradiated samples. The final values were expressed as percent of input $^{32}P$ counts per minute for noncovalent binding and for covalent photobinding were expressed as a percentage of noncovalent binding.

*Reverse-Phase HPLC Purification of T7 RNAP + 12MAf Photo-Cross-Linked Conjugate.* One milligram of T7 RNAP was mixed with approximately 138 μg of $^{3}H$ and $^{32}P$ labeled 12MAf in irradiation buffer in a final volume of 5 mL. The $^{3}H$ label (sp. radioact. = 17 000 Ci/mol) on the 12MAf was introduced by using $^{3}H$-HMT to prepare the MAf. The resulting $^{3}H$-12MAf was 5′ end labeled with the aid of [γ-$^{32}P$]-ATP and T4 polynucleotide kinase. The protein–DNA complexes were incubated at room temperature for 15 min and then irradiated with argon laser light by pumping the reaction mixture through a jacketed flow cell system as described previously (Spielmann et al., 1992) except that the reaction mixture was pumped through the flow cell only once (i.e., reactions were not "cycled"). The rate of pumping was ~5 mL/min. The flow system was washed twice with 5 mL of irradiation buffer to remove, as much as possible, any 12MAf–T7 RNAP complexes that remained in the flow cell system. These washes were added to the reaction mixture and the total reaction mixture (~15 mL) was dialyzed (MW cutoff of the dialysis membrane was 10 000) against a 133-fold excess of TE (10 mM Tris-HCl, pH 7.5, + 1 mM EDTA) for 24 h to remove most of the unbound DNA. Small aliquots (50 μL) of the irradiated mixture before and after dialysis were analyzed for covalent photo-cross-links by 12.5% polyacrylamide–SDS gel electrophoresis, to confirm the success of the large-scale irradiation. The volume of the large-scale T7 RNAP + 12MAf dialysate was reduced by lyophilization to 1.5 mL, and the complexes were separated on 12.5% polyacrylamide–SDS gels on a preparative scale. The covalent complexes were identified by autoradiography, excised from the gels, and isolated by electroelution. The eluted complexes were further purified on a C18 HPLC column (Rainin Instruments, Emeryville, CA) as follows. The DNA–protein complexes (~800 μg of protein) were made in 0.05% TFA and injected on to a Dynamax C18 column (4.6 mm i.d. × 25 cm length, 300 Å; 5 μm pore size) and eluted using the following gradient [similar to the one used by King et al. (1986)]: 0–90 min (0–37.5% B); 91–138 min (37.5%–75% B); 139–160 min (75–100% B). Buffer A was 0.05% TFA in water, and buffer B was 0.05% TFA in 80% acetonitrile. One-milliliter fractions were collected at a flow rate of 1 mL/min. To achieve optimal separation, several separate injections of the large-scale preparation were made. An aliquot (10 μL) from each fraction was assayed for $^{3}H$ and $^{32}P$ radioactivity with the addition of scintillation fluid. The peak fractions (112 and 113, Figure 8A) were lyophilized to dryness.

*Tryptic Digestion and Anion-Exchange HPLC.* The dried residue (~100 μg of protein) from reverse-phase HPLC was resuspended in 83.3 mM Tris-HCl, pH 8.0 + 1.6 mM $CaCl_2$ + 2 M urea. Trypsin (stock solution of 1 mg/mL in 10 mM HCl) was added in four aliquots at intervals of 15 h. The total amount of trypsin added was (27 μg) and the reaction was incubated at 37 °C for 72 h. The tryptic digest was then subjected to strong anion-exchange HPLC on a Rainin Hydropore-SAX (quaternary amine; column dimensions were 4.6 mm i.d. × 10 cm length) column to purify the DNA–peptide conjugates away from other peptides that did not contain the DNA oligo. The following conditions were used for strong ion-exchange HPLC (Chen et al., 1991). Buffer A: 50 mM Tris-HCl, pH 7.5, + 0.5 mM EDTA +10 mM 2-mercaptoethanol. Buffer B: 50 mM Tris-HCl, pH 7.5, + 0.5 mM EDTA + 10 mM 2-mercaptoethanol + 1 M NaCl. The gradient consisted of 0–5 min (0% B) and 6–65 min (0–100% B). One-milliliter fractions were collected at a flow rate of 1 mL/min. Aliquots (5 μL each) from each fraction were assayed for $^{3}H$ and $^{32}P$ with the addition of scintillation fluid.

Peak fractions (F1–F3, Figure 8B) from strong anion-exchange HPLC that contained the maximum amount of $^{3}H$ + $^{32}P$ radioactivity were repurified on a narrow-bore C8 reverse-phase column (Aquapore, 2.1 mm i.d. × 30 mm length; Applied Biosystems, Foster City, CA) by HPLC at the

Microchemical Facility (UC, Berkeley). Amino acid compositions of the peptides were determined at the Protein Structure Lab, UC, Davis.

*Transcriptional Cross-Linking.* The $^{32}$P-labeled template DNA was suspended in irradiation buffer supplemented with 35 units/50 $\mu$L of RNAse inhibitor (RNAguard, Pharmacia). To this solution, kept on ice, were added a mixture of rNTPs (ATP, CTP, GTP, UTP) to a final concentration of 500 $\mu$M each. The DNA solution was transferred from ice to a 37 °C water bath for 30 s. T7 RNAP was diluted in irradiation buffer + BSA (50 $\mu$g/mL final concentration) immediately before use. Transcription was initiated by the addition of T7 RNAP to 0.332 $\mu$M and continued for 5 min with incubation at 37 °C. The transcription reactions were then laser irradiated for 10 s (see Irradiation of Protein–DNA Reactions with a Continuous-Wave Argon Ion Laser section above). In some reactions, NaCl was added to 200 mM to prevent polymerase recycling (Sastry & Hearst, 1991a). The samples were treated as above before gel electrophoresis (see the Irradiation of Protein–DNA Reactions section). For quantitation of the transcripts, RNA was labeled with [$\alpha$-$^{32}$P]GpG as initiator on unlabeled DNA templates. Unlabeled GpG was supplemented to a final concentration with 750 $\mu$M in the transcription reaction. Initiation of GpG was done for 5 min before the addition of rNTPs, and transcription was continued for an additional 5 min. Promoter double-stranded templates were prepared by adding slight molar excess amounts of an 18 mer promoter top strand (5′-TAATACGACTCACTATAG-3′) to the 66 MAf bottom strand (see Figure 10).

## RESULTS

*Specific Photochemical Cross-Linking of DNA Binding Proteins to DNA Oligos Containing Psoralen Furanside Monoadducts.* Orren et al. (1992) first reported that UvrB protein can be photochemically cross-linked to a single-stranded DNA 12 mer or a 138 mer psoralen furanside monoadduct by irradiating the protein–DNA mixtures with 365-nm light from a low-power black ray lamp. In this work, we have extended this finding to a general method of cross-linking DNA binding proteins to DNA. We show that several single-stranded DNA binding proteins can be cross-linked to DNA oligos containing psoralen furanside monoadducts using an argon ion laser operating in the broad-band mode centered at 366 nm. In addition, we show that the T7 RNA polymerase in a ternary complex arrested at a furanside monoadduct can also be cross-linked to the template DNA by this method.

Figure 1 illustrates that four different proteins, T7 RNA polymerase (T7 RNAP, $M_r$ 98 856), UvrB ($M_r$ 76 118), RecA ($M_r$ 37 842), and T4 gene 32 ($M_r$ 33 487) protein can be cross-linked to a $^{32}$P-labeled 24 mer furanside monoadduct by irradiating the protein–DNA mixtures with argon ion laser light at 366 nm. For each protein (Figure 1), one can see at least two major bands as well as other minor bands, especially in an overexposed gel (Figure 1B). Larger amounts of RecA + 24MAf complexes were observed in the presence of ATP$\gamma$S than in the presence of ATP, because RecA–ssDNA noncovalent complexes are more stable in the presence of the nonhydrolyzable analogue (McEntee et al., 1981). No protein–DNA cross-linking was observed in the absence of laser light or in the presence of unmodified (non-psoralenated) 24 mer (Figure 1A,C). The same result was obtained with UvrB or RecA (data not shown). BSA, which is a non-DNA binding protein, did not cross-link to a 24MAf upon irradiation with laser light.

Cross-linking of T7 RNA polymerase to 12MAf was observed when the reactions were irradiated with laser light

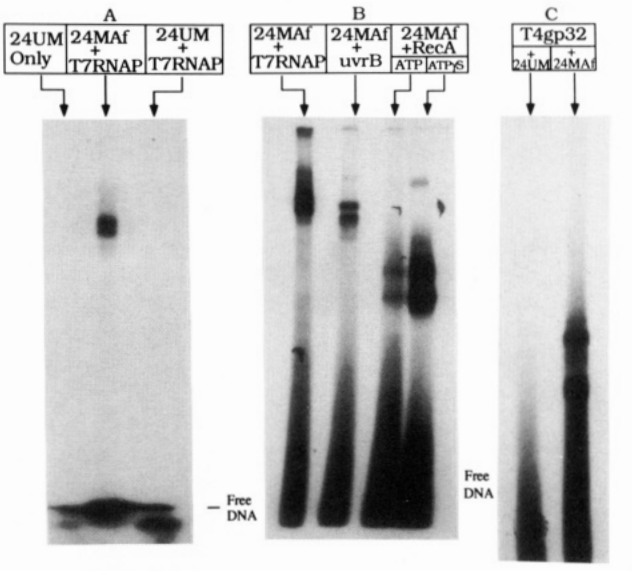


FIGURE 1: Laser-induced cross-linking of DNA-binding proteins to psoralenated DNA oligos. Several different DNA-binding proteins were mixed with purified single-stranded 24 mer DNA oligos containing a site-specific psoralen furanside monoadduct (24MAf) that was $^{32}$P end labled. The reaction mixtures were then irradiated with 366-nm laser light as described in Materials and Methods. The cross-linked proteins and DNAs were then run on SDS–polyacrylamide gels and the bands were visualized by autoradiography of the DNA. Protein–DNA cross-links appear as bands toward the top of the gels because of their retarded mobility compared to that of free DNA shown at the bottom of the gels. Panels A–C are autoradiograms of SDS–polyacrylamide gels. Each lane contained about 2.2 pmol of DNA and 2.6–10 pmol of proteins. ATP and ATP$\gamma$S were used at 1 mM final concentration in RecA reactions. Gels were exposed to X-ray film for different lengths of time to visualize fainter bands.

for 1 s. However, photoreactions for 10 s gave better yields. Prolonged irradiation times (30 s to 5 min) resulted in the loss of distinct gel bands representing cross-linked complexes. We therefore chose to irradiate the protein–DNA complexes for 10 s in all the experiments described in this paper.

We reproduced the results of Orren et al. (1992) under our reaction conditions by irradiating at 360–364 nm using a black ray lamp as a light source. Figure 2 shows that both T7 RNAP and UvrB were cross-linked to a 14 mer furanside monoadduct (14MAf; see Table I for the nucleotide sequence). In this experiment, we used relatively large amounts (200–300 pmol per lane) of proteins to visualize them by Coomassie Brilliant Blue staining of the gels following photoreaction. One major band and one or two additional faint bands of retarded mobility for each protein were seen in the autoradiogram. This is in contrast to the results with high intensity laser irradiation where overall greater amounts and more species of adducted proteins were found.

We think the presence of multiple bands in the lanes of the gels indicate isomers of the protein–DNA cross-links resulting from the reaction of the monoadducted DNA at multiple sites on the protein. Orren et al. (1992) did not observe multiple bands in the case of UvrB. Using a black light lamp similar to the one used by Orren et al., we observed the production of additional faint bands along with the major band. To develop these additional reaction products, we have used larger quantities of protein and DNA than those used by Orren et al. (1992) in both the reactions performed with the black light lamp and the more intense laser light source.

Staining the gels with silver or Coomassie blue showed no degradation of proteins following laser irradiation. No cross-linking of the proteins studied to radiolabeled unmodified DNA

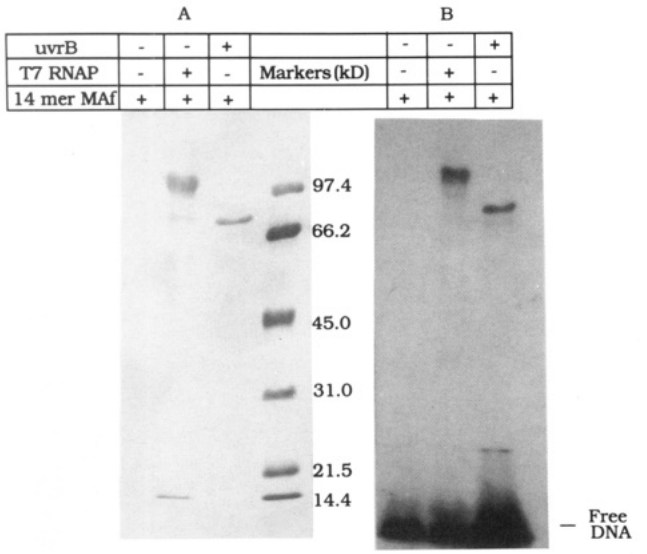


FIGURE 2: Cross-linking of proteins to DNA using black light radiation: 0.3 nmol of T7 RNAP was reacted with 0.1 nmol of $^{32}$P-14MAf; 0.2 nmol of UvrB was reacted with 0.25 nmol of $^{32}$P-14MAf. The lane where no proteins were present contained 0.1 nmol of $^{32}$P-14MAf. Panel A is a 10% SDS–polyacrylamide gel stained with Coomassie Brilliant Blue. Panel B is an autoradiogram of the same gel shown in panel A. The markers shown in the center lane are protein standards from Bio-Rad Laboratories. The wells of the comb used to cast this gel were wider than the wells used in the other figures of autoradiograms presented in this paper. The minor bands seen in the Coomassie-stained gel are products of protein degradation seen in nonirradiated protein samples also.

of identical sequence was seen in any of the reactions. We conclude that photo-cross-linking of the DNA to the protein is mediated by the psoralen on the DNA. Only the psoralen furanside monoadduct can be photoexcited at 366 nm by the monochromatic light source used to effect the photochemistry. We believe that these DNA–psoralen furanside monoadduct–protein interactions are covalent in nature because (a) the proteins are rigorously denatured by boiling in SDS and urea after the photoreaction; (b) the complexes cannot be competed away by the addition of 10X excess unlabeled monoadducted DNA oligo after the laser irradiation; and (c) the reaction is totally light-dependent.

Estimates of the amount of oligo covalently bound to the protein were done by scanning gels in a PhosphorImager. These estimates were carried out on gels where the labeled DNA did not run off the gel. At equimolar ratios of DNA/protein, ~2–5% of the input radiolabeled DNA was cross-linked to T7 RNAP, RecA (+ATPγS) and T4 gene 32 protein, including all the major bands after irradiation with laser light. In the case of UvrB, the amount of DNA cross-linked to the protein was only ~0.3–0.5% of the input DNA. These differences in cross-linking efficiencies may reflect differences in the noncovalent binding efficiencies between the various proteins to the DNA oligos.

In many gels the free DNA migrated as a long streak perhaps due to the SDS and/or salts in the samples. It is known that SDS and salts in the sample cause nonspecific aggregation of DNA resulting in artifacts in the mobility of DNA in gels.

*Measurement of Apparent Cross-Linking Constants.* Figures 3 and 4 show plots of the relationship of concentration of T7 RNAP or UvrB to the fraction of $^{32}$P-labeled 24MAf that was cross-linked to proteins in a series of laser-induced cross-linking experiments. The concentration of protein or the labeled oligonucleotide was increased in these experiments without changing the concentration of one or the other macromolecule. The fraction of bound DNA was calculated

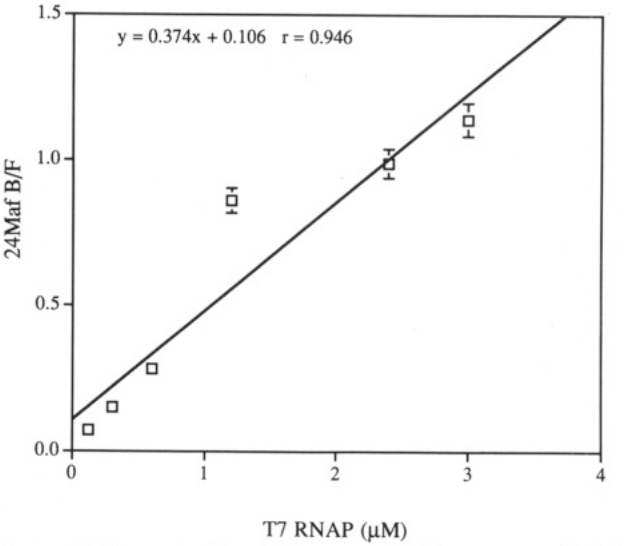


FIGURE 3: Determination of photo-cross-linking constant for T7 RNAP–24MAf conjugation. The graph was obtained by "fitting" the data points (not including the origin) using a linear regression equation (shown as inset). The Apple Macintosh Graph III computer program was used to generate the figure. Each data point represents the mean of two experimental values. The ordinate is the ratio of protein-bound MAf ($B$) to free MAf ($F$). All the reactions were subjected to laser irradiation at the same fluence (~$4.6 \times 10^{18}$ photons $s^{-1}$ $cm^{-2}$).

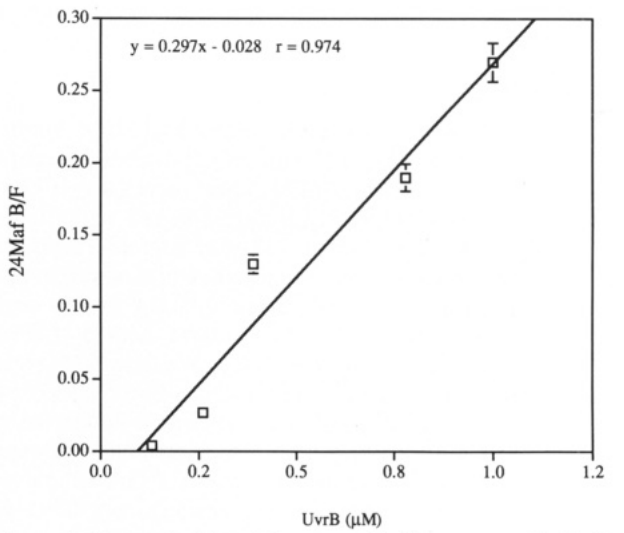


FIGURE 4: Determination of photo-cross-linking constant for UvrB–24MAf conjugation. The graph was obtained by "fitting" the data points (not including the origin) using a linear regression equation (shown as inset). Apple Macintosh Graph III computer program was used to generate the figure. Each data point represents the mean of two experimental values. The ordinate is the ratio of protein-bound MAf ($B$) to free MAf ($F$). All the reactions were subjected to laser irradiation at the same fluence (~$4.6 \times 10^{18}$ photons $s^{-1}$ $cm^{-2}$).

from the integrated peak areas of bands representing bound and free DNA on gels that were scanned in a PhosphorImager (gels are not shown). Each data point represents the mean of two experimental values. Increasing the concentration of proteins over those shown in Figures 3 and 4 resulted in a decrease in the yield of protein–DNA cross-links (data not shown). This decrease may be due to aggregation at high protein concentrations in the reaction mixture.

The straight lines in Figures 3 and 4 are least-squares fits of the data using a linear regression equation. The slopes of the lines give the apparent cross-linking constants ($K_{appXL}$) for the respective proteins which were $3.74 \times 10^{-7}$ M for T7 RNAP and $2.97 \times 10^{-7}$ M for UvrB. The cross-linking

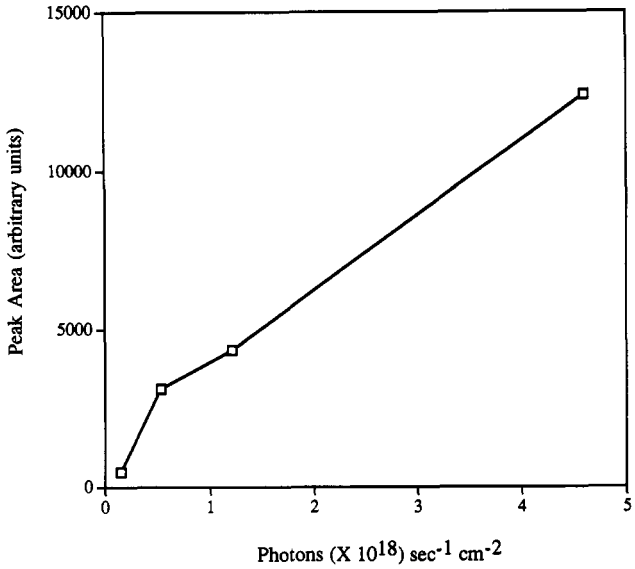


FIGURE 5: Cross-linking as function of increasing laser light fluence. The total photon flux was varied by changing the power output of the laser but keeping the sample exposure times constant. The ratio of $^{32}P$ labeled 24MAf DNA to T7 RNAP was constant at 1:3 in each lane. Data points were obtained from a gel subjected to autoradiography using a PhosphorImager.

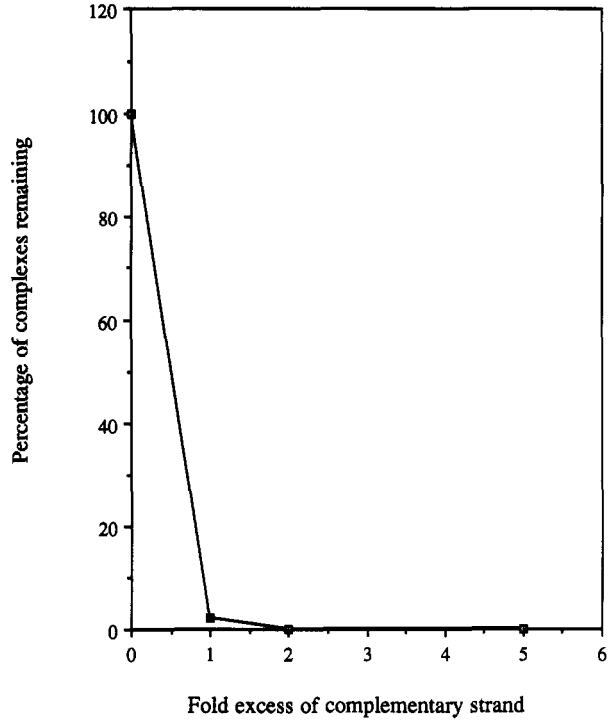


FIGURE 6: Effect of the addition of unlabeled 24 mer complementary DNA strand on cross-linking of $^{32}P$ labeled 24MAf to T7 RNAP. $x$-axis indicates the molar-fold increase in complementary strand as compared to the $^{32}P$ labeled 24MAf present. T7 RNAP was added to a mixture of the two DNA strands, and the reactions were subjected to laser irradiation at the same fluence ($\sim 4.6 \times 10^{18}$ photons $s^{-1}$ $cm^{-2}$). The amount of complexes in the absence of the complementary strand is represented at 100%, and the amounts of complexes remaining after each addition of complementary strand are expressed relative to 100%. Each reaction contained 3 pmol of T7 RNAP and 12 pmol of $^{32}P$ labeled 24MAf. Data points were obtained from a gel subjected to autoradiography using a PhosphorImager.

constant for T7 RNAP that we determined is in agreement with the equilibrium binding constant with T7 promoter DNA previously reported by two independent groups. The binding constant of T7 RNAP for a class III promoter was calculated to be (2–4) $\times 10^{-7}$ M by Gunderson et al. (1987) and by Sousa et al. (1992). On the other hand, Ikeda and Richardson (1987) reported a much weaker equilibrium binding constant with the same promoter DNA, viz., $2 \times 10^{-5}$ M, under different experimental conditions. The nonspecific binding constant of T7 RNAP with a 32-bp nonpromoter DNA was estimated to be $1 \times 10^{-5}$ M. Since the experimental conditions and the sequence of the monoadducted nonpromoter single-stranded DNA used here are completely different from those used by other workers, comparisons are not strictly valid.

In the presence of UvrA and ATP, the $K_{eq}$ for UvrB–DNA (thymine-dimer) complex formation was reported to be 0.7 $\times 10^{-9}$ M (Orren & Sancar, 1990). No previously published binding constants for T7 RNAP or UvrB complexed with psoralenated DNA are available for comparison.

*Effect of Increasing Laser Light Intensity on Cross-Link Formation.* Increasing fluences of laser light at a fixed molar ratio of protein/24MAf resulted in almost a linear increase in the amount of cross-link product (Figure 5). The yield of cross-links is represented as the integrated peak areas ($y$-axis) of the bands corresponding to the protein–DNA cross-links scanned by PhosphorImage analysis of the gels (Figure 5). The data are plotted as a function of the laser fluence ($x$-axis). Figure 5 shows that the yield of cross-links is completely light-dependent.

*Cross-Linking of Protein to MAf Is Absent in the Presence of the Complementary DNA Strand.* There was a drastic decrease in laser-induced cross-linking of protein to radiolabeled 24MAf when increasing amounts of complementary DNA strand were added to $^{32}P$-24MAf and then incubated with T7 RNAP. Figure 6 shows a dose-dependent decrease in the amount of T7 RNAP–24MAf cross-link as a function of increasing amount of unlabeled complementary 24 mer unmodified strand. The addition of an equimolar amount of complementary strand to the radiolabeled 24MAf single strand resulted in the formation of only a small fraction of the amount of protein–DNA complexes that were formed in the absence of the complementary strand (taken to be 100% in Figure 6). Additional amounts of complementary strand resulted in complete loss of T7 RNAP + $^{32}P$-24MAf cross-link formation. The absence of cross-link formation is in part due to the low affinity of T7 RNAP to (nonpromoter) dsDNA oligos compared to that of ssDNA (Muller et al., 1988; Sousa et al., 1992) and partly to competing reactions of interstrand DNA cross-linking. Analysis of $^{32}P$ labeled DNA on 8 M urea–PAGE after laser irradiation showed the presence of only interstrand DNA cross-links between MAf and the complement (not shown).

Table I: Furanside Monoadducted DNA Oligos Used in This Work[a]

| | | |
|---|---|---|
| 1. | 5′-TCG**T**AGCT-3′ | 8 mer |
| 2. | 5′-GAAGC**T**ACGAGC-3′ | 12 mer |
| 3. | 5′-CGAAGC**T**ACGAGCA-3′ | 14 mer |
| 4. | 5′-GATCCCCGGG**T**ACCGAGCT-3′ | 19 mer |
| 5. | 5′-GATCGCTCCCGGG**T**ACCGAGCTCG-3′ | 24 mer |
| 6. | 5′-AGTCACGACGTTGTAAAACGACGGC-CAGTGAATTCGAGCTCGG**T**ACCCGG-3′ | 50 mer |

[a] The site of monoaddition is the T with an asterisk in the TpA shown in bold. All the oligos except the 50 mer were synthesized by a new procedure described by Spielmann et al. (1992). The 50 mer was synthesized by Cheng et al. (1991).

*Cross-Linking of Proteins to MAf Occurs Irrespective of DNA Sequence and Length.* Table I shows the different furanside DNA oligos used in this work. The sequences are

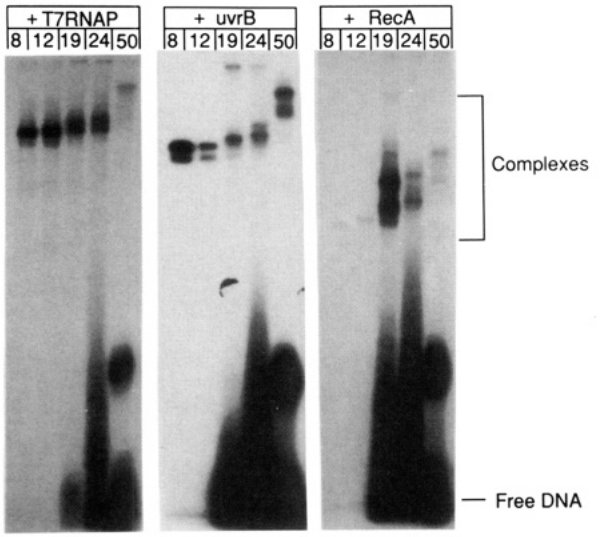


FIGURE 7: Cross-linking of proteins to oligo MAfs of different length and nonspecific sequence. Different lengths of $^{32}P$ labeled MAfs were mixed with indicated proteins at approximately the same molar ratios and irradiated with laser light at the same fluence ($\sim 4.6 \times 10^{18}$ photons $s^{-1}$ $cm^{-2}$). The molar ratio of DNA to protein was $\sim$1:0.5 for T7 RNAP and RecA. For UvrB, the molar ratio was 1:0.8. Autoradiograms were exposed to films for different lengths of time in order to visualize the faint bands. The numbers at the top indicate the length (nucleotides) of the oligos. See Table I for the nucleotide sequences. The shortest oligos (8 and 12 nts) completely ran off the gels. The large oval spot three-fourths of the way down the gel in the lanes containing the 50 mer could represent an intrastrand cross-link.

not related except that they are generally G+C rich and A+T-deficient, to promote the site-specific photochemical addition of psoralen (Gamper et al., 1984). A single 5′-TpA-3′ where the monoadduct is situated is common to all of the oligos. Figure 7 presents the results of laser cross-linking of T7 RNAP, UvrB, and RecA (+ATPγS) to the different oligo MAfs in the size range of 8 mer to 50 mer. Cross-linking of T7 RNAP, UvrB, and RecA (+ATPγS) occurs with all oligomer MAfs tested (Figure 7). These differences in cross-linking efficiency may reflect differences in noncovalent binding of the proteins to the oligo MAfs (see below). In the case of T7 RNAP and RecA (+ATPγS) reaction with 8 mer oligo MAf, the predominant product of cross-linking is one band. Some minor bands are also visible on overexposed gels. Increasing the length of the oligo MAf up to 50 nucleotides results in the presence of at least two major bands with both T7 RNAP and RecA (+ATPγS). On the other hand, with UvrB at least two prominent bands are consistently seen irrespective of the length of the oligo MAf. We believe the appearance of multiple bands for a given oligo + protein photoreaction signifies the presence of multiple sites on the protein for oligo MAf cross-linking. Each band may represent a separate isomer of the protein as a result of the oligo cross-linking to a different site on the polypeptide. These results suggest that there are at least two major sites for cross-linking on the proteins studied. In the case of T7 RNAP and RecA (+ATPγS), when the length of the oligo is quite small (8 nts) the majority of the photochemical cross-linking is directed to one site as represented by the presence of a single band on the denaturing gel. When the length of the oligo increases, cross-linking occurs at a minimum of two sites on the protein as represented by the appearance of two bands. Two sites are available for cross-linking to UvrB irrespective of the length of the oligo, although there appears to be a preferred site as indicated by the relative intensities of the two bands. We present more definitive evidence for multiple cross-linking sites obtained by extensive HPLC purification of tryptic digests of 12MAf DNA–T7 RNAP conjugates.

Table II: Binding of Furanside Monoadducts to Different Proteins

| oligo Maf | T7RNAP non-covalent[a] | T7RNAP co-valent[b] | UvrB non-covalent[a] | UvrB co-valent[b] | RecA non-covalent[a] | RecA co-valent[b] |
|---|---|---|---|---|---|---|
| 8 mer | 1.5 | 60.5 | 1.7 | 21.1 | 1.9 | 5.5 |
| 19 mer | 9.1 | 7.3 | 10.1 | 7.9 | 8.2 | 13.3 |
| 50 mer | 32.5 | 0.6 | 82.8 | 0.7 | 71.3 | 0.8 |

[a] Calculated as the percent of input $^{32}P$-oligo bound to protein. [b] Calculated as the percent of noncovalent binding. The details of the nitrocellulose filter binding assay for covalent and noncovalent protein–MAf complexes are in the Materials and Methods section. Each value is an average of duplicates from two separate experiments. The molar ratios of DNA/MAf were 1:0.5 for T7 RNAP and RecA, and for UvrB it was 1:0.8. Note that it has been previously reported that UvrB is not a DNA binding protein (Thomas et al., 1985). However, those studies were conducted with an $\sim$4-kbp plasmid. With small ssDNA, there is some nonspecific binding as reported by Orren et al. (1992).

*Covalent Photobinding as a Fraction of Noncovalent Binding.* Table II shows the results of a filter-binding assay for protein binding to a set of MAfs of different lengths. Covalent photo-cross-linking was examined as a function of noncovalent protein binding. In the cases of T7 RNAP and UvrB, there is an inverse relationship between covalent photobinding and noncovalent binding as the length of the MAf increases. With RecA, this is true only in the case of 50 mer. RecA + 8MAf consistently gave lower noncovalent and covalent photobinding than T7 RNAP and UvrB. The poor binding of RecA to 8MAf is in agreement with the finding that stable RecA binding to single-stranded DNA does not occur with very short oligonucleotides (McEntee, 1981). In a series of reaction of a protein with MAf oligos of different lengths, the highest reactivity was observed for the shortest oligos. With 8MAf + T7 RNAP or UvrB, a high percent of these noncovalent sites is converted to covalent sites by the laser. Increasing the length of the MAf increases the total amount of noncovalent protein binding to the oligo, perhaps due to cooperative binding. As the MAf length increases, a decreasing fraction of these protein-bound DNA molecules undergoes photo-cross-linking. This is most likely because only one or two protein molecules in the complex are in direct contact with the psoralen monoadduct irrespective of the number of noncovalently bound protein molecules on any one DNA molecule. The fraction of protein binding sites on an oligo that contain a monoadduct is proportionately smaller for longer pieces of DNA. As a result, only a small fraction of the noncovalent interactions is converted to a covalent adduct by the laser light for the longest oligo MAf tested.

*HPLC Purification of Covalent T7 RNAP + 12MAf Conjugates.* Isolation of a large amount of the T7 RNAP + 12MAf conjugates was the first step to demonstrate that multiple sites for photo-cross-linking of the oligo MAf exist on T7 RNAP, and to localize the various cross-linking sites on the protein. This was achieved in several successive steps which included preparative gel electrophoresis and HPLC purification. A large-scale reaction mixture of T7 RNAP + 12MAf was irradiated and run on preparative SDS–polyacrylamide gels to separate non-cross-linked DNA from protein-bound DNA. The protein–DNA complexes were recovered from the gel slices by electroelution. The eluted complexes were further purified by reverse-phase HPLC on C18 columns. We observed some spontaneous protein degradation in the T7 RNAP + 12MAf preparation during handling prior to HPLC purification. We attribute the random cleavage of the protein following irradiation to the following

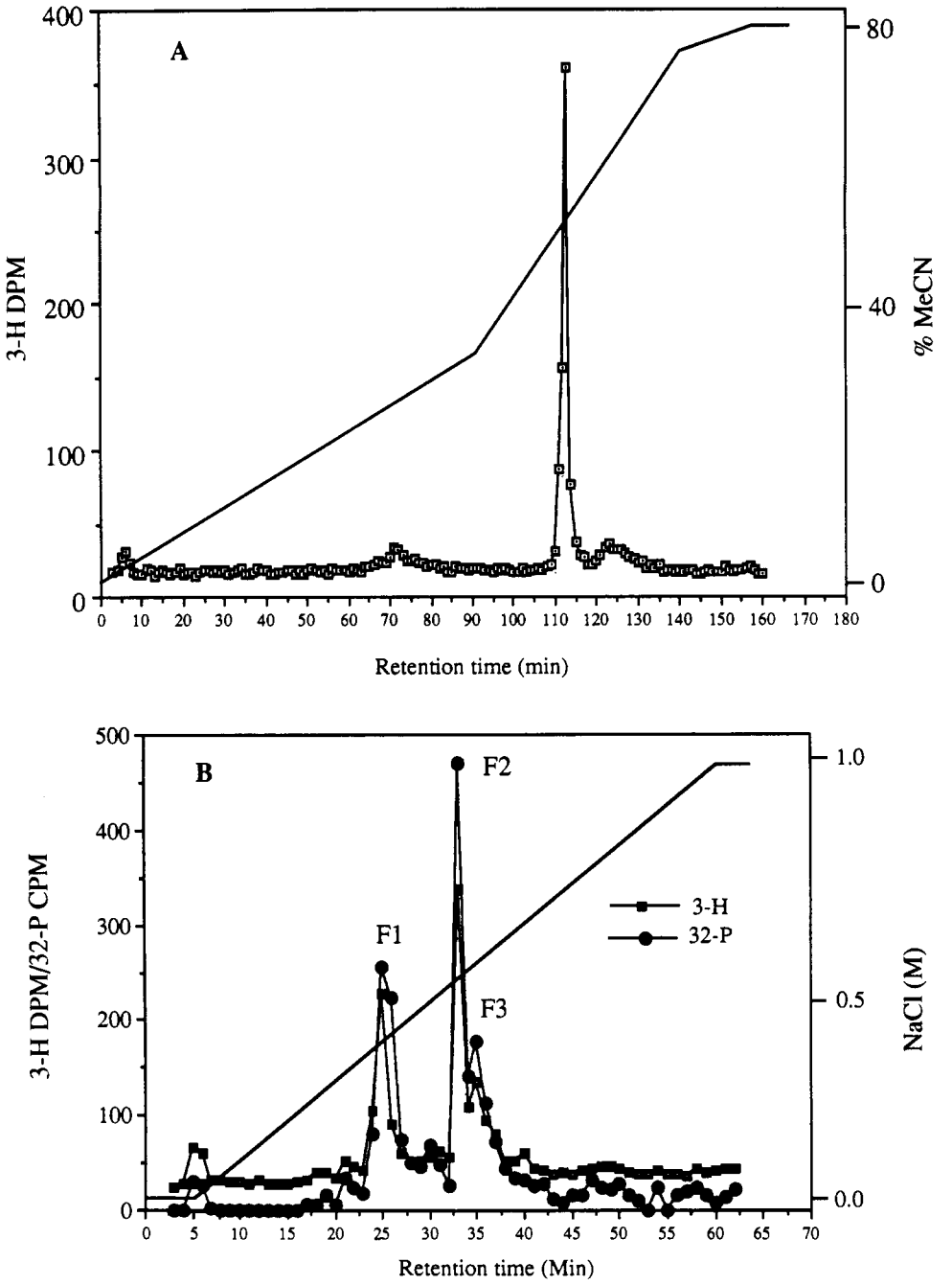


FIGURE 8: HPLC purification of covalent T7 RNAP + 12MAf conjugates. (A) Reverse-phase C18 column purification of T7 RNAP + 12MAf conjugate(s) (~200 μg of protein/injection) that were first isolated from preparative SDS–polyacrylamide gels. (B) Strong anion-exchange chromatography of tryptic digests of reverse-phase purified T7 RNAP + 12MAf conjugate(s). Details of the procedures are given in Materials and Methods. The 12MAf DNA was double-labeled before the photoreactions to monitor the elution of only the peptide–DNA conjugate. The $^{3}H$ label is on the HMT monoadduct, and the $^{32}P$ label is on the 5′ end of the DNA. The shapes of the gradients are indicated by the lines. F1–F3 are peak fractions that were analyzed.

reasons. The T7 RNAP + 12MAf large-scale preparation was found to migrate as an intact protein species at ~100 kDa immediately following laser irradiation and dialysis, indicating no direct cleavage of the protein. However, some spontaneous cleavage was observed after prolonged (4 days) storage of the preparation at −20 °C and subsequent cycle of freeze–thawing and lyophilization to dryness. The harsh denaturing sample preparation conditions for gel electrophoresis and reverse-phase HPLC conflicted with conditions that stabilize protein integrity (such as high concentrations of glycerol, moderate concentrations of salts, and storage at −20 °C). These conditions included taking up the irradiated T7 RNAP + 12MAf samples in aqueous TFA at low pH (~1.5–2.0) for reverse-phase HPLC. Previous reports have documented degradation of proteins following UV-A irradiation of protein + free psoralen mixtures (Veronese et al., 1982). It appears that some spontaneous degradation of protein following photochemistry is unavoidable during adduct purification using the current methodology.

Figure 8A shows the $^{3}H$ elution profile of a single round of C18 reverse-phase HPLC purification of electroeluted complexes. The psoralen in the 12MAf was labeled with tritium. T7 RNAP containing the cross-linked 12MAf elutes as a single sharp peak. The optical trace of the elution pattern (not shown) monitored at $A_{230nm}$ showed that the peak fractions (nos. 112 and 113) eluted in a sharp peak without any shoulders, thus attesting to its homogeneity. Other minor peaks (Figure 8A) were discarded. The $^{32}P$ profile (not shown

in Figure 8A) exactly coincided with the $^3H$ profile indicating that this peak contained the MAf DNA oligo. When a laser-irradiated sample of 12MAf alone (i.e., without T7 RNAP) was run on C18 HPLC under the same buffer gradient conditions used here, the DNA oligo was not appreciably retained by the column and came off in the void volume (e.g., 5 and 6 min; e.g., see Figure 8A). These results indicate that the major peak of radioactivity shown in Figure 8A is the result of peptides or protein bound to 12MAf and not simply 12MAf alone or its photo-damaged products. Peak fractions (nos. 112 and 113, Figure 8A) were lyophilized and extensively digested with trypsin. To isolate only the peptides covalently bound to the DNA away from other peptides that were not bound to DNA, we took advantage of the strong affinity of DNA to quaternary amine columns (Hydropore-SAX, Rainin Instruments). Figure 8B shows that tryptic digestion of the T7 RNAP + 12MAf conjugates resulted in three major peaks containing radioactivity (F1–F3). Estimation of the relative amounts of DNA and protein content of F1–F3 fractions by taking the $A_{260}/A_{280}$ ratio revealed approximate DNA/protein mass ratios of 2, 3, and 1 for F1–F3, respectively. Estimation of the DNA content in F1–F3 fractions based on the amount of $^3H$ label in each of the fractions and the specific radioactivity of the $^3H$ also agreed with the above ratios. The three peak fractions (F1–F3) from SAX–HPLC were subjected to photoreversal of the DNA–psoralen linkage by a brief (2-min) exposure to 254-nm UV light from a germicidal lamp. This treatment normally causes photoreversal of the psoralen–DNA cyclobutane ring. Since we do not understand the chemical nature of the laser-induced peptide–psoralen cross-link in our system, we do not know if the psoralen-peptide cross-link was stable to the 254-nm UV photoreversal. Since this treatment was only for a very brief period of time, we do not anticipate any UV 254-nm-induced peptide–DNA cross-linking. This photoreversal step was undertaken in an attempt to ameliorate the failure of our initial attempts to sequence the DNA–peptide conjugates by automated Edman sequencing. We reasoned that the presence of the covalently attached DNA on the peptide somehow hindered the sequencing of the peptides. The photoreversed F1–F3 fractions were further purified individually by C8 narrow-bore reverse-phase HPLC to isolate individual peptides. C8 reverse-phase HPLC of each fraction from SAX–HPLC (F1–F3) revealed one major peak and several minor peaks indicating the heterogeneity of each of the SAX fractions. The major peaks from the narrow-bore reverse-phase HPLC had different retention times (HPLC profiles not shown). The major peak from F1 had a retention time of 46.3 min, the major peak from F2 had a retention time of 42.3 min, and the major peak from F3 had a retention time of 54.8 min.

*Localization of the MAf Cross-Linking Region in the T7 RNAP Amino Acid Sequence.* Several attempts to determine the amino acid sequence of F1–F3 major peptides by automated gas-phase Edman sequencing methodology failed. This failure was not for lack of sufficient quantities of these peptides. Optical HPLC traces and estimation of protein concentration using the bicinchoninic acid protein assay indicated that these modified peptides were available in microgram quantities. There are at least two possible reasons for the failure to obtain sequence information: (a) The modified conjugated sample was not efficiently retained by the polybrene-coated support used in gas-phase automated sequenators; (b) the N-termini were not accessible to the sequencing methodology (see Discussion).

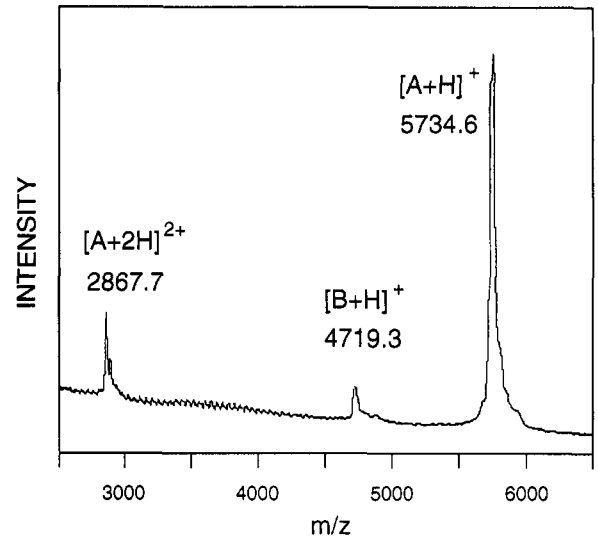


FIGURE 9: Matrix-assisted laser desorption mass spectrum of the major peptide from the F1 fraction. The region shown contains singly ($m/z$ 5734.6) and doubly ($m/z$ 2867.7) charged ions of bovine insulin [A] as standard. The $m/z$ 4719.3 of singly charged species [B] of F1 peptide is indicated. Details of the procedure used to acquire the mass spectrum are given in Beavis and Chait (1990).

Matrix-assisted ultraviolet laser desorption mass spectrometry (Beavis & Chait, 1990)[2] of the major peptide in the F1 fraction revealed a mass of 4719 amu (Figure 9). Pulses from a frequency tripled Nd-YAG laser operating at 355 nm were used to produce sample desorption. Psoralen monoadducts absorb light at 355 nm and are susceptible to photoreactions at this wavelength. Because the chemical nature of the psoralen–peptide bond is unknown, it is unclear whether the laser desorption procedure maintains the integrity of the linkage. It is also possible that the psoralen–peptide linkage was photoreversed when the sample was exposed to 254-nm light to remove the nucleic acid. It is unlikely that this mass corresponds to an unmodified peptide.

The amino acid composition of the F1 fraction indicated that there were no histidines in the F1 fragments. A tryptic peptide map from the known amino acid sequence of T7 RNAP (Dunn & Studier, 1981; Moffat et al., 1984) was generated using the PEP program from Intelligenetics Corporation's (Mountain View, CA) computer software. With the peptide map as a guide, we scanned the sequences of the various candidate peptides using the following constraints: (1) The amino acid composition of the fragment should not contain a histidine. (2) The mass of the candidate peptide fragment should be close to the determined mass for the F1 peptide. (3) There should be no internal cleavable tryptic sites in the sequence of the fragment, assuming that the covalently linked DNA did not protect the protein from trypsin digestion. There is only one region of T7 RNAP that meets these criteria. This fragment spans residues 558–608 with a MW of 5459. Within this sequence, there are two trypsin-resistant (Wilkinson, 1986) sites at 576–578. This fragment falls within the putative DNA (promoter) binding domain, i.e., the C-terminal one-third of the T7 RNAP sequence, as deduced from point mutation studies (Joho et al., 1990; Bonner et al., 1992, and references therein). We predict that the F1 peptide may be a subfragment that arose from this region. Since F1 contained other minor peptides besides the major peptide used for mass determination, the amino acid composition of the predicted peptide fragment

[2] Determined in the laboratory of Dr. Brian T. Chait at The Rockefeller University, New York City.

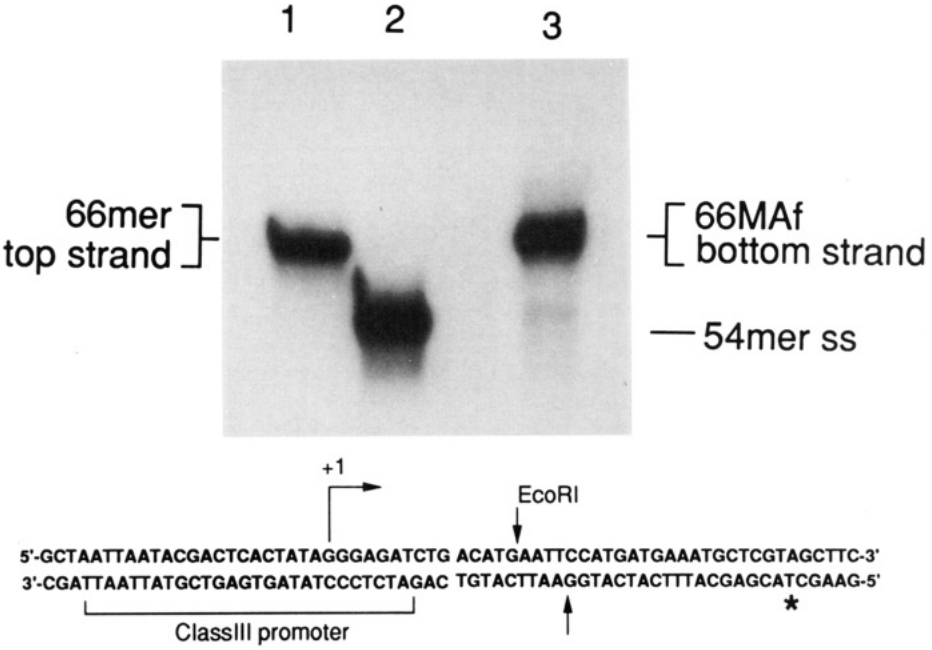


FIGURE 10: Construction of a HMT monoadducted T7 RNAP template. Unlabeled 12 MAf was ligated to a 5′ $^{32}$P labeled 54 mer bottom strand (lane 2). The products of the ligation (a 66MAf) are shown in lane 3. The $^{32}$P label is present internally on the bottom strand (lane 3) as a result of ligation. Lane 1 shows a 5′ $^{32}$P end labeled sample of a purified top strand DNA. A slight molar excess of top strand and $^{32}$P labeled bottom strand were mixed and heat-cooled to obtain a labeled ds 66MAf template for transcription. The sequence of the template and the position of the HMT furanside monoadduct (asterisk) are shown below. +1 indicates the transcription start site.

cannot be directly matched with the determined amino acid composition of F1.

Amino acid compositions for the F2 and F3 fractions were not be determined. We expended most of the material from the F2 and F3 major peptides in futile attempts at sequence determination, and we did not have sufficient amounts of peptide to perform amino acid analysis on these fractions.

*Usefulness of the Procedure To Generate Cross-Linked T7 RNAP Elongation Complexes at a Unique Site on the DNA Template.* In previous reports (Shi et al., 1988; Sastry & Hearst, 1991a,b), we showed that stalled elongation complexes of T7 RNAP can be generated by placing a psoralen furanside monoadduct or cross-link downstream of a promoter on a DNA template. As shown in Figure 10, we constructed a T7 RNAP template bearing a class III promoter and site-specific monoadduct at +38 on the bottom strand as indicated by an asterisk. Briefly, a 12MAf was ligated to a 54 mer [as in Sastry and Hearst (1991a)] to prepare a 66MAf template strand (Figure 10). A synthetic 66 mer unmodified complementary strand was added to the 66MAf template strand to obtain a double-stranded 66MAf template for transcription. We used three different derivatives of the 66MAf template strand to test the efficiency of T7 RNAP transcription and laser-induced cross-linking of the elongated T7 RNAP to the DNA templates. The results are shown in Figure 11. No cross-linking of the template to T7 RNAP was seen with single-stranded 66MAf. On the other hand, both the promoter double-stranded and the fully double-stranded templates were cross-linked to T7 RNAP (Figure 11). Analysis of the $^{32}$P-labeled transcripts (with [$\alpha$-$^{32}$P]GpG as initiator) showed that the single-stranded template was transcriptionally inactive, whereas the partially double-stranded and the fully double-stranded templates supported transcription by T7 RNAP and indeed produced the expected +37 and secondary +38 nucleotide transcripts [see Sastry and Hearst (1991a)]. This result demonstrates that the appearance of T7 RNAP + DNA cross-links indeed coincided with the production of appropriate transcripts on the templates. Addition of 200 mM NaCl after 5 min of transcription to prevent promoter binding and recycling of the polymerase [see Sastry and Hearst (1991)], did not result in a change in the amount of cross-linking (Figure 11). No cross-links were detected in the absence of NTPs or T7 RNAP (data not shown), indicating that the cross-links are the result of elongation of T7 RNAP to the site of the monoadduct on the template strand. Specific labeling of the RNA transcript with $^{32}$P did not reveal cross-links between the RNA and the (ds)DNA template after the laser cross-linking reaction. The lack of such cross-links can be interpreted as the nascent RNA adopting a geometry in the ternary complex that is incompatible with DNA–psoralen–RNA cross-linking.

Two major protein–DNA cross-link bands along with other minor bands are seen on the gels (Figure 11). Quantitation of all the bands representing the cross-links by PhosphorImagery indicated that ~2–5% of the $^{32}$P-labeled DNA template was cross-linked to T7 RNAP when either a partially or fully double-stranded template was used. Multiple bands on SDS–PAGE (Figure 11) indicated multiple sites for cross-linking of the T7 RNAP to the DNA. The accessibility of different sites on the arrested T7 RNAP for cross-linking to the DNA template implied that the arrested polymerase molecules may exist in multiple conformations with respect to the geometry of the DNA template. This is probably because the arrested polymerase is in a dynamic flux as shown previously by a DNaseI footprinting assay [see Sastry and Hearst (1991a)]. We observed that more than 80% of the cross-links were due to interstrand DNA cross-links when a fully double-stranded template was used to cross-link T7 RNAP to the DNA. Using *Eco*RI or RNaseH as a diagnostic tool to detect cross-linked ds DNA or DNA–RNA hybrids, respectively, we found that with a fully dsDNA template the majority of photo-cross-links were interstrand DNA cross-links (data not shown). No cross-links that represented RNA–DNA hybrids were detected when the cross-linked $^{32}$P-template was treated with RNaseH. DNA–DNA cross-links and any RNA–DNA cross-links have retarded mobility on an 8 M urea denaturing gel. There is

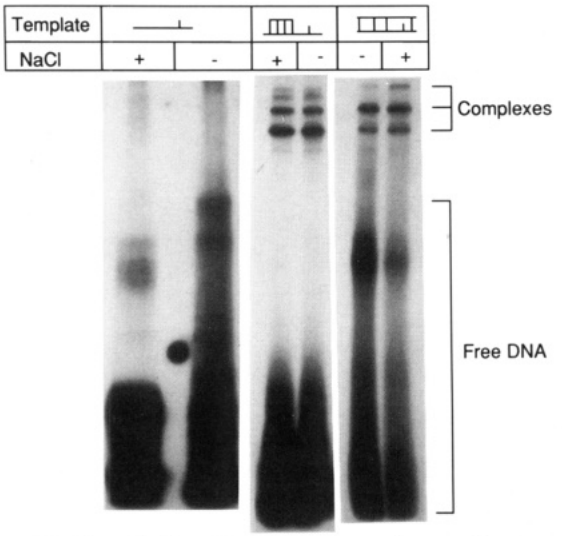


FIGURE 11: Cross-linking of T7 RNAP elongation complexes arrested at the HMT adduct site on a monoadducted template. The conformations of the templates are indicated above in the boxes. The DNA templates were labeled internally with $^{32}P$ on the bottom strand as described in legend to Figure 9. The two parallel lines in the top box indicate top and bottom strands. Vertical lines indicate base pairing of the two strands of the template DNA. The small vertical spike on the bottom strand signifies the HMT monoadduct. Bands toward the top of the gel designated as complexes are T7 RNAP–template cross-links. Each lane contained approximately 0.86 nmol of template DNA.

an *Eco*RI restriction site near the middle of the template DNA. Treatment of the cross-linked molecules with *Eco*RI gives fragments that run with greater mobility than the parent cross-linked molecule. If there were cross-linked RNA–DNA hybrids, the RNA component would be chewed up by the RNaseH treatment, resulting in loss of material from the slower moving cross-linked nucleic acid band. There was no loss of cross-linked material when the sample was treated with RNaseH.

## DISCUSSION

*Cross-Linking Technique.* In this report, we have extended the work of Orren et al. (1992) by demonstrating the formation of adducts between T7 RNA polymerase and its DNA template in a ternary complex arrested at a furanside monoadduct and by cross-linking several single-stranded DNA binding proteins to DNA MAfs of different lengths via the psoralen furanside monoadduct. In principle, this technique can be used to probe DNA–protein contacts in situations where the DNA double helix is unwound by DNA tracking proteins (helicases, polymerases, repair enzymes, etc.). Cross-linking of RNA binding proteins to furanside monoadducts could also be achieved, provided that sufficient amounts of synthetic monoadducted RNAs can be manufactured. The present method is superior to traditional UV (254-nm) cross-linking techniques because unlike the latter, protein–DNA cross-linking can be directed to a certain specific region of a DNA by site-specifically placing a monoadduct on the DNA substrate. Multiprotein complexes, such as those in eukaryotic transcription complexes, assembled on psoralen monoadducted DNA substrates may also be amenable to probing with the technique we have presented here. The question of which individual protein or proteins in a multiprotein ensemble is in direct contact with a subsequence of the target DNA can be answered using this cross-linking technique. This may provide information about the interrelationship between different proteins or subunits in a multiprotein complex.

The use of lasers to achieve DNA–protein cross-linking is clearly advantageous compared to traditional low power lamps [see also Hockensmith et al. (1991); Harrison et al., 1982]. The time of irradiation is drastically reduced from 30 min–1 h with traditional lamps to a few seconds in this procedure. The highly monochromatic laser light is only absorbed by the psoralen monoadduct, not by the protein or the DNA being probed. The photochemical efficiency of the cross-linking process is improved by the use of high light flux. Pulse lasers (at ~365 nm) could also be used to effect protein–MAf cross-links, although we suspect that substantial degradative chemistry may follow cross-linking because of the generally high peak powers of the pulses. Laser-induced cross-linking is rapid (nanoseconds to milliseconds) compared to the time scale of equilibrium association–dissociation rates (seconds to minutes) of most protein–nucleic acid interactions in vitro (Record et al., 1978). This technique offers a method of "freezing" the "instantaneous" binding equilibria in the reactions. With appropriate modifications, the laser cross-linking technique we have described here could be used to study the kinetic and thermodynamic aspects of protein–DNA interactions and DNA–DNA interactions (e.g., secondary structures such as hairpins and triple helices) with psoralenated oligos.

*Multisite Cross-Linking Model.* The cross-linking events have probably occurred through different amino acids in the protein. Veronese et al. (1982) showed that free psoralen photoreacted with several different amino acids, such as His, Trp, Tyr, Met, and Pro in lysozyme. It is likely that DNA-bound monoadducted psoralens will also react with different amino acids. In our system, it remains to be shown which amino acids are involved in the cross-linking interactions.

The evidence in favor of more than one reactive site between an oligo and the same protein is the presence of multiple bands on denaturing analytical gels. In the case of 254-nm UV-induced protein-DNA cross-linking, instances where more than one amino acid in the same protein was cross-linked with the oligonucleotide have been documented [see Williams and Konigsberg (1991) for review]. In human A1 hnRNP, several Phe residues were involved in cross-linking to a DNA oligo (Merrill et al., 1988). Webster et al. (1992) found that regA protein of bacteriophage T4 cross-linked to $(dT)_{16}$ at Phe-106 as well as at Cys-36 in different proteolytic peptides. Similarly, Cleghon and Klessig (1992) found that both Met-299 and Phe-418 were cross-linked to a synthetic DNA in adenovirus DNA binding protein. In ribonucleaseA–(pUp) cross-links, three different amino acids have been shown to be involved in cross-linking (Havron & Sperling, 1977).

Because of the low overall photochemical cross-linking yield, there is no more than one oligonucleotide cross-linked to any one protein molecule. After treatment of the complex with trypsin, we observe more than one species of peptide–DNA cross-link. We believe that this is due to multiple binding sites for the MAf on the protein. The variation in the relative amounts of cross-linked peptides is due to a difference in the populations of the complexes modulated by the reactivity of the MAf in its respective binding site. These modified peptides may arise from different conformations of the protein–DNA complex.

*Chemistry of Protein–MAf Cross-Linking.* Two mechanisms can be discussed in relation to the photobinding of psoralens to proteins: (1) Singlet oxygen ($^1O_2$) (Poppe & Grossweiner, 1975; de Mol et al., 1981) and radicals or radical ions (Cannistraro & van de Vorst, 1977; Schiavon & Veronese, 1984); (2) direct photobinding (Midden, 1988). Several

groups have reported that the photochemical interaction of psoralens with proteins is oxygen-sensitive and $^1O_2$ plays a role in the adduct formation (Veronese et al., 1981, 1982; Granger et al., 1982; Morliere et al., 1986; Singh & Vadasz, 1978). Singlet oxygen quenchers such as $NaN_3$ (Foote, 1984) reduced the amount of protein–psoralen adduct formation, while $D_2O$, which increases the lifetime of $^1O_2$ by 10-fold (Kearns, 1984), enhanced adduct formation (Veronese et al., 1981, 1982; Granger et al., 1982; Morliere et al., 1986; Singh & Vadasz, 1978). But the magnitude of enhancement of adduct formation in $D_2O$ was much smaller compared to what one would expect on the basis of $^1O_2$ lifetime. The effects of these additives on cross-linking are complex and cannot be taken to prove the existence of $^1O_2$ mediation. This is because the magnitude of the rate enhancements in the presence of $D_2O$ are a combination of sensitizer triplet quantum yields and SΔ ratio, rate constant for $^1O_2$ reaction with substrates, and other solvent effects (Midden, 1988). Mechanisms that do not invoke $^1O_2$ in the reaction of psoralens with amino acids have also been considered. These may involve direct photobinding and radical or radical ion-mediated reactions (Yoshikawa et al., 1979; Muller-Runkel & Grossweiner, 1981; Veronese et al., 1981, 1982; Schiavon & Veronese, 1986; Midden, 1988).

In contrast to the work cited above where free psoralens were used, we have used DNA oligos with psoralen furanside monoadducts. Photoexcited furanside monoadducts are also known to produce $^1O_2$ (de Mol et al., 1981). In our system, the results on the effects of $NaN_3$ and $D_2O$ on cross-linking were complex. In experiments comparing the amounts of cross-linking between T7 RNAP or UvrB or RecA (+ATPγS) and 24MAf in $D_2O$ (80% v/v) vs $H_2O$, we observed only a slight (1.5–2.7-fold) increase in the amount of cross-link in $D_2O$ as compared to $H_2O$ (data not shown). But the increase in noncovalent binding in $D_2O$ vs $H_2O$ was also comparable: ~1.5-fold increase in noncovalent binding in $D_2O$ as compared to $H_2O$. Similarly, $NaN_3$ (at 0.5% w/v; 26 mM $Na^+$) not only reduced (2-fold) covalent cross-linking but also inhibited noncovalent binding. These results indicated that, in our cross-linking system, whatever increase or decrease in covalent cross-linking in the presence of these additives was likely due to the corresponding changes in the observed noncovalent binding which precedes cross-linking.

We did not conduct any cross-linking experiments under deoxygenated conditions, partly because a number of published reports have already indicated that the photoreactivity of psoralens to proteins under deoxygenated conditions reduced the yield of cross-links by at least an order of magnitude compared to oxygenated conditions (Yoshikawa et al., 1979; Veronese et al., 1981; Schiavon et al., 1984) and partly because of the technical difficulties involved in deoxygenating enzymatic reactions conducted in small volumes (50 μL) in Eppendorf tubes.

*Possible Reasons for the Inability to Sequence the Peptides.* Our failure to sequence the cross-linked peptides was a surprising result. In our Edman sequencing reactions we observed a relatively high background of amino acids in the first few cycles of sequencing, followed by a sharp drop in the level of amino acids without further appearance of an amino acid sequence in the subsequent sequencing cycles. Since the amount of peptides loaded on to the membrane support were sufficiently high (50–100 pmol), the simplest explanation was that the sample was not efficiently absorbed onto the polybrene-coated support. This problem has been encountered by others who have attempted to sequence DNA-conjugated peptides in automated gas-phase sequenators (Prof. Kenneth R. Williams, personal communication). The other possibility that the N-terminus of the peptide is somehow blocked or inaccessible to the coupling reaction cannot be ruled out.

The cross-linked amino acid residue(s) may not be regenerated from the adduct after acid hydrolysis during amino acid composition analysis, thus making it impossible to correctly identify the amino acid(s) involved in cross-linking. Also, these modified amino acids could have quite different retention times on chromatographic columns compared to some known standards of modified amino acids. Isolation of tryptic peptides of ribonucleaseA that was directly photoreacted with free psoralen has been reported (Schiavon et al., 1984). These authors attributed their difficulties in obtaining amino acid sequence information to the extreme heterogeneity of the photomodified peptides. Amino acid composition of the modified protein was used to deduce the cross-linked residues solely on the basis of the loss in the amounts of certain amino acids recovered after acid hydrolysis.

*Cross-Linked T7 RNAP Elongation Complexes.* The ability to generate stable cross-linked elongation complexes of T7 RNAP with a psoralen monoadducted DNA template should help facilitate the characterization of these complexes by physicochemical approaches such as NMR and X-ray crystallography.

When a fully double-stranded template was used to cross-link T7 RNAP to the template, we observed that most of the template DNA (>80%) was cross-linked (interstrand DNA cross-links) and only a small amount of the template was cross-linked to protein (Figure 11). No cross-links that represented RNA–DNA hybrids were detected when either a $^{32}P$-labeled RNA transcript was isolated or the cross-linked material from a $^{32}P$-labeled DNA template was treated with RNaseH. These results confirm our earlier suggestion [see Sastry and Hearst (1991a)] that unwinding of the two DNA strands of the template does not occur past the psoralen in the "bubble" of the ternary complex arrested at the psoralen. Otherwise, such a high degree of interstrand DNA cross-linking would not have occurred. The lack of RNA–DNA cross-links also indicates that the growing point (3′-OH nucleotide) of the nascent RNA is not accessible for photochemistry by the monoadduct on the template strand, because it is either somehow sequestered by the enzyme or spatially separated from the psoralen on the double-stranded template. We believe that the laser-induced cross-linking occurs in the intact arrested T7 RNAP complex because the entire experiment takes place during the estimated "dwell time" of the arrested T7 RNAP which is in the order of 10–13 min [see Sastry and Hearst (1991a)].

## ACKNOWLEDGMENT

We thank Dr. Tariq Rana for advice and suggestions during the early part of the experimental work and Dr. Chris Noren for the T7 RNA polymerase. Special thanks to Dr. Claus Schneider in Prof. Brian Chaits's Lab at The Rockefeller University (New York) for his efforts with the mass spectrometry of the peptides.

## REFERENCES

Beavis, R. C., & Chait, B. T. (1990) *Anal. Chem. 62*, 1836–1840.

Bonner, G., Patra, D., Lafer, E. M., & Sousa, R. (1992) *EMBO J. 11*, 3767–3775.

Budzik, G. P., Lam, S. M., Schoemaker, H. J. P., & Schimmel, P. R. (1975) *J. Biol. Chem. 250*, 4433–4439.
Cannistraro, S., & van de Vorst, A. A. (1977) *Biochim. Biophys. Acta 467*, 166–177.
Chen, L., MacMillan, A. M., Chang, W., Ezaz-Nikpay, K., Lane, W. S., & Verdine, G. L. (1991) *Biochemistry 30*, 11018–11025.
Cheng, S., Sancar, A., & Hearst, J. E. (1991) *Nucleic Acids Res. 19*, 657–663.
Cimino, G. D., Gamper, H., Isaacs, S. T., & Hearst, J. E. (1985) *Annu. Rev. Biochem. 54*, 1151–1193.
Cleghon, V., & Klessig, D. F. (1992) *J. Biol. Chem. 267*, 17872–19881.
de Mol, N. J., Henegouwen, B. G. M. J., & van Beele, B. (1981) *Photochem. Photobiol. 34*, 661–666.
Dunn, J. J., & Studier, W. F. (1983) *J. Mol. Biol. 166*, 477–535.
Foote, C. S. (1984) in *Singlet Oxygen* (Wasserman, H. H., & Murry, R. W., Eds.) pp 139–171, Academic Press, New York.
Gamper, H. B., Piette, J., & Hearst, J. E. (1984) *Photochem. Photobiol. 40*, 29–34.
Gorelic, L. (1975a) *Biochim. Biophys. Acta 390*, 209–225.
Gorelic, L. (1975b) *Biochemistry 14*, 4627–4633.
Granger, M., Toulme, F., & Helene, C. (1982) *Photochem. Photobiol. 36*, 175–180.
Gunderson, S. I., Chapman, K. A., & Burgess, R. R. (1987) *Biochemistry 26*, 1539–1546.
Harrison, C. A., Turner, D. H., & Hinkle, D. C. (1982) *Nucleic Acids Res. 10*, 2399–2414.
Havron, A., & Sperling, J. (1977) *Biochemistry 16*, 5631–5635.
Hillel, Z., & Wu, G. W. (1978) *Biochemistry 17*, 2954–2961.
Hockensmith, J. W., Kubasek, W. L., Vorachek, W. R. Evertsz, E. M., & von Hippel, P. H. (1991) *Methods Enzymol. 208*, 211–236.
Ikeda, R., & Richardson, C. C. (1987) *J. Biol. Chem. 262*, 3800–3808.
Joho, K. E., Gross, L. B., McGraw, N. J., Raskin, C., & McAllister, W. T. (1990) *J. Mol. Biol. 215*, 31–39.
Kearns, D. (1984) in *Singlet Oxygen* (Wasserman, H. H., & Murry, R. W., Eds.) pp 115–137, Academic Press, New York.
King, G. C., Martin, C. T., Pham, T. T., & Coleman, J. E. (1986) *Biochemistry 25*, 36–40.
Kunkel, G. R., & Martinson, H. G. (1978) *Nucleic Acids Res. 5*, 4263–4272.
Laemmli, U. K. (1970) *Nature 227*, 680–683.
Lica, L., & Ray, D. S. (1977) *J. Mol. Biol. 115*, 45–59.
Maniatis, T., Fritsch, E. F., & Sambrook, J. (1982) *Molecular Cloning—A Laboratory Manual*, Cold Spring Harbor Laboratory, Cold Spring Harbor, NY.
Markovitz, A. (1972) *Biochem. Biophys. Res. Commun. 281*, 522–534.
McEntee, K., Wienstock, G. M., & Lehman, I. R. (1981) *J. Biol. Chem. 256*, 8835–8844.
Merrill, B. M., Williams, K. R., Chase, J. W., & Konigsberg, W. H. (1984) *J. Biol. Chem. 259*, 10850–10856.
Merrill, B. M., Stone, K. L., Cobianchi, F., Wilson, S. H., & Williams, K. R. (1988) *J. Biol. Chem. 263*, 3307–3313.
Midden, W. R. (1988) in *Psoralen DNA Photobiology* (Gasparro, F. P., Ed.) Vol. 2, pp 16–49, CRC Press, Boca Raton, FL.
Moffatt, B. A., Dunn, J. J., & Studier, F. W. (1984) *J. Mol. Biol. 173*, 265–269.
Moller, K., & Brimacombe, R. (1975) *Mol. Gen. Genet. 141*, 343–355.
Morliere, P., Cremer, J., Toulme, J. J., Santus, R., & Dubertret, L. (1986) *Photochem. Photobiol. 44*, 425–431.
Muller, D. K., Martin, C. T., & Coleman, J. E. (1988) *Biochemistry 27*, 5763–5771.
Muller-Runkel, R., & Grossweiner, L. I. (1981) *Photochem. Photobiol. 33*, 339–402.
Musajo, L., & Rodighiero, G. (1972) in *Photophysiology* (Giese, C., Ed.) p 115, Academic Press, New York.
Orren, D. K., & Sancar, A. (1990) *J. Biol. Chem. 265*, 15796–15803.
Orren, D. K., Selby, C. P., Hearst, J. E., & Sancar, A. (1992) *J. Biol. Chem. 267*, 780–788.
Paradiso, P. R., & Konigsberg, W. (1982) *J. Biol. Chem. 257*, 1462–1467.
Pathak, M. A., & Fitzpatrick, T. B. (1992) *J. Photochem. Photobiol. B 14*, 3–22.
Poppe, W., & Grossweiner, L. (1975) *Photochem. Photobiol. 22*, 217–219.
Reboud, A. M., Buisson, M., Marion, M. J., & Reboud, J. P. (1978) *Eur. J. Biochem. 90*, 421–426.
Record, M. T., Jr., Anderson, C. F., & Lohman, T. M. (1978) *Q. Rev. Biophys. 11*, 103–178.
Sastry, S. S., & Hearst, J. E. (1991a) *J. Mol. Biol. 221*, 1091–1110.
Sastry, S. S., & Hearst, J. E. (1991b) *J. Mol. Biol. 221*, 1111–1125.
Sastry, S. S., Spielmann, H. P., Dwyer, T. J., Wemmer, D. E., & Hearst, J. E. (1992) *J. Photochem. Photobiol. B 14*, 65–79.
Schiavon, O., & Veronese, F. M. (1986) *Photochem. Photobiol. 43*, 243–246.
Schiavon, O., Simonic, R., Ronchi, S., Bevilacqua, R., & Veronese, F. M. (1984) *Photochem. Photobiol. 39*, 25–30.
Schwartz, D. C., Saffran, W., Welsh, J., Haas, R., Goldberg, M., & Cantor, C. R. (1983) *Cold Spring Harbor. Symp. Quant. Biol. 47*, 189–195.
Shetlar, M. D. (1981) in *Photochemical & Photobiological Reviews* (Smith, K. C., Ed.) pp 105–196, Plenum Press, New York.
Shetlar, M. D., Christensen, J., & Hom, K. (1984) *Photochem. Photobiol. 39*, 125–133.
Shi, Y.-B., Gamper, H., & Hearst, J. E. (1988) *J. Biol. Chem. 263*, 527–534.
Singh, H., & Vadasz, J. A. (1978) *Photochem. Photobiol. 28*, 539–545.
Smith, K. C. (1977) in *The Science of Photobiology* (Smith, K. C., Ed.) Plenum Press, New York.
Sousa, R., Patra, D., & Lafer, E. M. (1992) *J. Mol. Biol. 224*, 319–334.
Spielmann, H. P., Sastry, S. S., & Hearst, J. E. (1992) *Proc. Natl. Acad. Sci. U.S.A. 89*, 4514–4518.
Strniste, G. F., & Smith, D. A. (1974) *Biochemistry 13*, 485–492.
Thomas, D. C., Levy, M., & Sancar, A. (1985) *J. Biol. Chem. 260*, 9875–9883.
Veronese, F. M., Schavon, O., Bevlacqua, Bordin, F., & Rodighiero, G. (1981) *Photochem. Photobiol. 34*, 351–354.
Veronese, F. M., Schavon, O., Bevlacqua, Bordin, F., & Rodighiero, G. (1982) *Photochem. Photobiol. 36*, 25–30.
Webster, K. R., Keill, S., Konigsberg, W., Williams, K. R., & Spicer, E. K. (1992) *J. Biol. Chem. 267*, 26097–26103.
Wilkinson, J. M. (1986) in *Practical Protein Chemistry—A Handbook* (Darbre, A., Ed.) John Wiley & Sons Ltd., Chichester.
Williams, K. R., & Konigsberg, W. H. (1991) *Methods Enzymol. 208*, 516–539.
Yoshikawa, K., Mori, N., Sakakibara, S., Mizuno, N., & Song, S. (1979) *Photochem. Photobiol. 29*, 1127–1133.